A systematic analysis of the dynamics of microwave- and conventionally-assisted swing adsorption on zeolite 13X and an activated carbon under post-combustion carbon capture conditions.

Yassin, M.[a], Biti, S.[a], Afzal, W.[a,b], Martín, C.F. [a,b (*)]

[a] University of Aberdeen, School of Engineering, Fraser Noble Building, King's College, Aberdeen AB24 3UE, Scotland, United Kingdom

[b] Centre for Energy Transition, University of Aberdeen

[(*)] Corresponding author: cfmartin@abdn.ac.uk

Abstract

This work presents a detailed parametric experimental work on the feasibility of microwave regeneration of two commercial adsorbents in a dynamic carbon capture swing adsorption system. A synthetic flue gas (15 % v/v CO_2 in N_2) dry or with (15 % relative humidity) was selected, along with Norit R2020CO2 activated carbon and 13X zeolite. A purpose-modified experimental apparatus was used to compare microwave-assisted and conventional thermal swing regeneration. The impact of operating parameters on the dynamic process performance was measured for microwave and conventional heating. Parameters considered were type of adsorbent, flue gas composition, CO_2 capture capacity, recovery, purity, quantity of adsorbent (and bed size), desorption kinetics, and time of full regeneration. Results showed that microwave-assisted regeneration presents advantages over its conventional equivalent, as CO_2 purity, recovery, and productivity were found to be higher under the former for the two adsorbents studied. For the time needed to achieve 50, 80, 90, and 99 % regeneration, the benefits of microwave regeneration over conductive regeneration increased with an increase in sample size. Under the wet gas feed, Norit R2020CO2 and zeolite 13X showed an appreciably higher working capacity with microwave regeneration than with conventional regeneration (39.68 and 24.23 % higher, respectively). Under the dry gas feed, the two adsorbents also maintained a higher working capacity with microwave heating as opposed to conductive heating (9.36 and 20.39 % higher,

respectively). The larger working capacity observed with microwave-assisted regeneration is attributed to the better regeneration.

Keywords: CO_2 capture, microwave heating, thermal heating, desorption kinetics, activated carbon, zeolite, thermal swing adsorption, microwave swing adsorption

1. Introduction

The increased use of fossil fuels witnessed in the last few decades is largely attributable to rapid global economic growth that has intensified the consumption of energy extracted from fossil fuel sources such as coal, oil, and natural gas. A major consequence of such escalated fossil fuel combustion has been the release of large volumes of anthropogenic greenhouse gas emissions such as CO_2, which by this means accounted for 90 % of total CO_2 emissions in 2015 [1]. The CO_2 levels in the atmosphere have grown at 2 ppm per year on average in the last ten years, and currently stand at 40 % higher than in the mid-1800s [1]. There is a clear positive correlation between rising atmospheric CO_2 concentrations and increasing average global temperature [2]. The 4th and 5th assessment reports issued by The Intergovernmental Panel on Climate Change (IPCC) confirmed that global warming is connected to increased greenhouse gas concentration. The report asserted that CO_2 emissions must be reduced by 41-72 % to maintain the global temperature rise under 2 ^{0}C by 2050 and avoid irreversible environmental impacts due to climate change [3]. One of the main mitigation strategies proposed in reducing atmospheric CO_2 levels is Carbon Capture, Utilisation and Storage (CCUS). The IPCC'S latest report (IPCC AR6) published this year (2021) also reaffirmed the findings in the 5th assessment report (AR5) [4].

The IPCC estimated that CCUS could contribute to 15-55 % of total climate change mitigation efforts by 2100 [3]. In addition to that, a study conducted by the International Energy Agency (IEA) concluded that without CCS, the cost of achieving a 50 % reduction in the global CO_2 emissions will be 70 % higher [5]. CCUS however entails added costs to current energy production activities. The most developed and deployed amine scrubbing process (capture by absorption) to date has characteristic barriers to implementation such as intensive solvent regeneration energy, high solvent losses and

degradation, and equipment corrosion [6]. An alternative to the absorption process of removing CO_2 from flue gas is an adsorption-based technology that uses solid sorbents. Among CCUS technologies, post-combustion carbon capture by means of adsorption offers potential energy savings to the deployment of carbon capture units that can process and convert low concentrated CO_2 flue gas into high CO_2 purity gas streams, suitable for CO_2 utilisation and/or storage [7].

The most consolidated practical approaches to achieve gas separation with solid sorbents are cyclic adsorption-regeneration processes conducted within a thermal swing (TSA, from thermal swing adsorption), a pressure swing (PSA, from pressure swing adsorption), or the combination of both (PTSA). Although TSA is one of the most investigated swing adsorption processes, its main limitation is the high energy penalty associated with the adsorbent regeneration, thus making the capture process less cost-effective [8]. The latter is considered as one of the main barriers to CCUS implementation. Accordingly, this study investigates a unique and transformative technology that uses an unconventional heating source (microwave energy) for the adsorbent regeneration in a cyclic post-combustion swing adsorption carbon capture process.

The beneficial aspect of microwave regeneration over conventional regeneration lies in the different mechanisms in which the two-heating processes proceed. Heat capacity, heat conductivity, and heat diffusivity of the adsorbent determine the flow and final distribution of heat within the bed in the thermal swing adsorption process (TSA). Initially, the direction of heat flow is from the surface into the core of the adsorbent until equilibrium is achieved. Low heat conductivity could lead to a large temperature gradient through the bed. In the case of microwave heating, the adsorbent's dielectric constant (ε') and loss factor (ε'') dictate how well the electromagnetic radiation is absorbed and converted into heat. The creation of a temperature gradient in microwave heating is minimal as the whole adsorbent receives radiation at the same instant. The volumetric heating nature of microwaves allows for the delivering of energy directly into the pores where CO_2 is adsorbed, overcoming the adsorption energy.

Microwave-assisted regeneration of solid sorbents: state-of-the-art

A newly reported work by Meloni *et al.* claimed that they have achieved a 75 % energy efficiency with microwave regeneration of 13X compared to conventional thermal regeneration. They also found an excellent repeatability in terms of CO_2 adsorption and desorption [9]. Bougie *et al.* worked on non-aqueous MEA solutions for CO_2 capture. With diethylene glycol monoethyl ether (DEGMEE), they found a 78 % reduction in energy consumption compared to the conventional 30 wt % MEA aqueous solution, as well as substantial cyclic CO_2 capture capacity under microwave regeneration [10]. Vacuum swing regeneration (VSR) assisted with microwave heating was studied by Webley and Zhang using wet and dry flue gas (12 % v/v CO_2 in N_2) and zeolite 13X as adsorbate and adsorbent respectively. It was found that CO_2 purity in the outlet stream was enhanced by 20 % due to the addition of MW heating in the system. When the flue gas was wet, the temperature increase was found to be much lower than predicted upon MW heating, suggesting that water was mainly responsible for the microwave absorption and subsequent temperature rise [11].

A study conducted by Foo and Hameed focused on regenerating durian shell and jackfruit peel-based activated carbons loaded with methylene blue dye (MB) [12]. The team used microwave irradiation for 3 and 4 minutes to regenerate the activated carbons. After performing five adsorption-regeneration cycles, the adsorption uptake and carbon yield were found to be stable, and the structural integrity of the materials remained unaffected by microwave heating. Several adsorbents (silica, activated alumina, NaX, and NaY zeolites) with different textural and dielectric properties were exhausted with various adsorbates (water, toluene, n-heptane, and methylcyclohexane) and regenerated with microwave heating as reported by Polaert *et al.* They found that both the MW power employed, and the dielectric properties of the adsorbates and adsorbents were more important than the molecular and porous structure of the adsorbate and adsorbent respectively. The group asserted that the polarity of the adsorbate is crucial as it assists the initial conversion of the absorbed power into heat [13]. Recent work performed by Chen *et al.* on beaded activated carbon derived from recycled waste bamboo tar also showed promising potential for microwave heating application in adsorbent regeneration. Over 93 % of adsorbate (methylethylketone and toluene) removal was achieved in 8 minutes with microwave radiation (power used: 600 W) [14].

The applicability of microwave energy on adsorbate desorption was explained by Lv *et al.* [15], where toluene adsorbed on a surface-modified NaY zeolite in a humid environment (relative humidity of 50 %) was desorbed with microwave heating. On top of achieving efficient regeneration, the adsorption capacity was kept stable after five adsorption-desorption cycles. In an effort to enhance adsorption capacity and microwave regeneration rate, the group mixed the modified zeolite with activated carbon in a 30/70 (carbon/zeolite) proportion. The composite adsorbent was regenerated efficiently with microwave heating, having achieved a substantial increase in capacity compared to the modified NaY on its own.

The heat transfer during microwave-assisted desorption was investigated by Ito *et al.* who used water vapour and a zeolite-packed bed as adsorbate and adsorbent, respectively. The study compared the conventional heating efficiency when heating the bed with only hot air, versus microwave heating combined with hot air. They concluded that the heating, and therefore the desorption rate, was much higher when the hot air heating is combined with microwave heating as opposed to hot air heating only. The study also suggested that microwave heating is fast and effective from the beginning [16]. A reasonable regeneration of granulated activated carbon (GAC) exhausted with chemical wastewater was achieved under microwave heating in research conducted by Liu *et al.* Exactly 400W of microwave power for 3 minutes was found to be the optimal conditions to restore 97.6 % of the initial adsorption capacity of 10 g of the GAC. However, after repeated cycles, a decrease in surface area and increase in surface basicity was observed, accompanied by a fall in adsorption capacity and 10 % adsorbent weight loss. Finally, their economic analysis evaluation suggested that the total cost of microwave energy needed for regeneration is about 24.3 % of GAC price at a pilot scale [17].

This work investigated the feasibility of microwave-assisted swing regeneration for post-combustion carbon capture and its advantages over the traditional temperature swing regeneration. This was done by carrying out a comparative study between the two regeneration techniques. Experiments were conducted with two commercial adsorbents: Activated carbon and a zeolite with a simulated feed gas from coal-fired power plants, representative of post-combustion flue gas, both pre-cleaned (dry gas) and wet (i.e. containing 15 % of relative humidity, RH). The effects of the two regeneration techniques

on key process parameters such as the adsorbent's working capacity, CO_2 regeneration extent, productivity, purity, and recovery were evaluated and compared. To the best of our knowledge, such a comprehensive comparison between these two regeneration techniques has not been conducted on these adsorbents for this post-combustion carbon capture separation process at these selected conditions. Hence the outcome of this work will broaden the technological alternatives to the existing adsorption-based carbon capture technologies.

2. Materials, experimental procedure, and methods

2.1. Adsorbents and gases

Norit R2030CO_2 (referred to as Norit R): a commercial activated carbon provided by Cabot Corporation. Norit R is an extruded, steam-activated, peat-based carbon with 2-3 mm particle diameter. It is specifically designed for CO_2 removal. Zeolite 13X (referred to as 13X): 13X is a commercial faujasite type zeolite (Si/Al ~1.0–1.4) with high sodium cation density in its framework [18] that was purchased from Alfa Aesar. It is a pellet-form molecular sieve with 1-2 mm particle diameter. Gases used in the MWSA/TSA studies were CO_2, N_2, and He, all ultrahigh purity and research-grade gases (99.995-99.998 %) were provided by BOC UK.

2.1.1. Material characterisation

The sorbents were characterised with different techniques to obtain physical and chemical attributes relevant to gas adsorption/desorption in the thermal swing adsorption process. N_2 adsorption/desorption isotherms at -196 °C were measured in a Micromeritics Tristar 3000 V5.00. Prior to any measurement, the samples were outgassed with N_2 at 300 °C with a heating rate of 3 °C/min for approximately 12 h. The BET surface area (S_{BET}), total pore volume (V_p), and pore size distribution (PSD) were determined from the N_2 isotherms at -196 °C. The surface area was calculated using the Brunauer-Emmett-Teller (BET) equation, and the total pore volume (V_p) was calculated from the adsorbed nitrogen after complete pore condensation at p/p0 = 0.9905 by applying Gurvich's rule [21]. PSD was calculated using density functional theory (DFT)- slit pore and NLDFT equilibrium model. Chemical characterisation was performed by point of zero charge- pH_{PZC}, and elemental analysis (CHNS).

2.2. Experimental apparatus

The experimental apparatus which includes the main adsorption unit used for this study is shown in Figure 1. The details of each unit within the experimental apparatus are reported in our previous work [19].

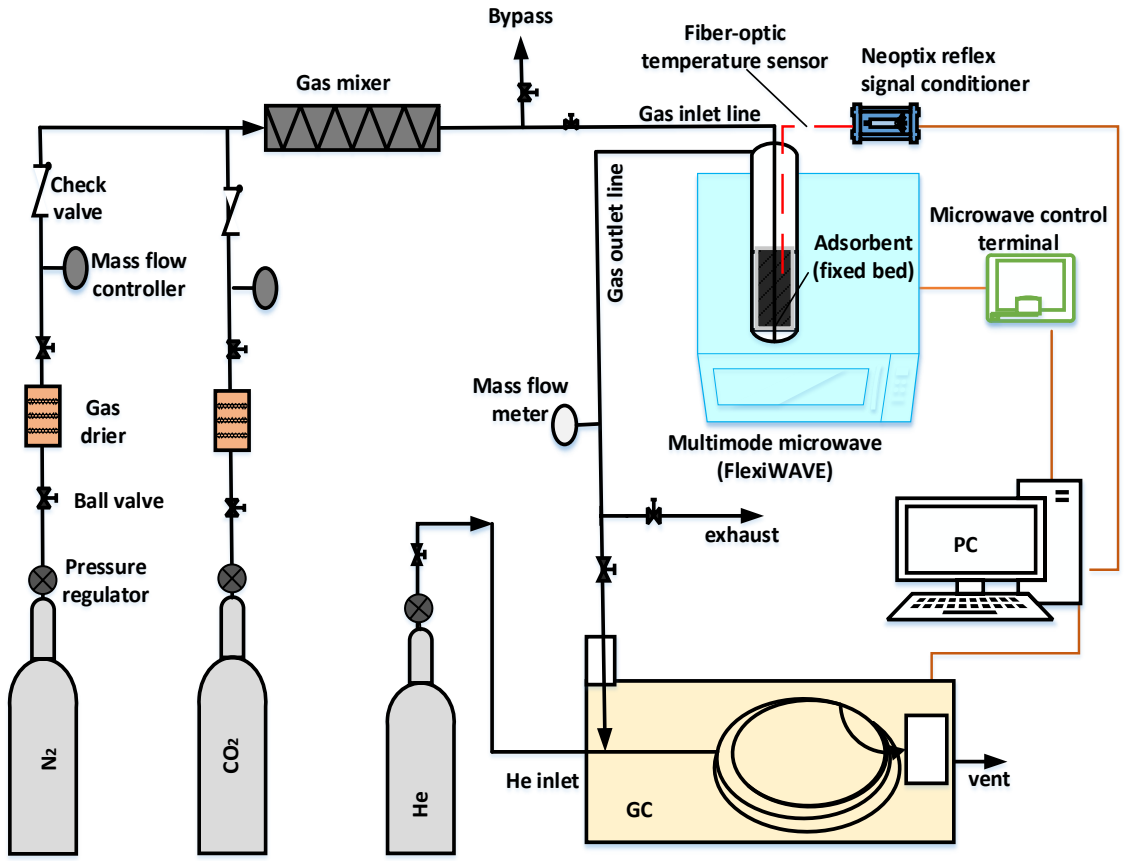

Figure 1. Experimental apparatus showing the main adsorption unit and the rest of the components.

2.3. Dynamic TSA and MWSA cycles

2.3.1. Experimental procedure

CO_2 adsorption capacity at dynamic conditions was measured from the breakthrough curves for the selected adsorbents (cycles with saturation). Experiments were performed in the adsorption unit shown above (Figure 1). For the unsaturated cycles, the adsorption process was stopped just before the breakthrough time (pre-determined, fixed time based on the breakthrough time for each adsorbent). In

a typical experiment, the reactor was packed with 6 g of adsorbent (or 48 g) and the following steps were executed:

Out-gassing (pre-conditioning): In a representative cyclic adsorption-desorption experiment, prior to adsorption, the samples were out-gassed overnight at 300 °C (13X) and 250 °C (Norit sample) with 20 NmL/min N_2 gas flow in an electric Nabertherm tube furnace (RT 50-250/11) equipped with a PID controller. The heating rate was set at 3 ^{0}C/min from the ambient temperature. The out-gassed sample was then weighted in a Fisher-brand scale (FAS64, readability 0.0001 g), and loaded into the reactor.

Purging: After placing the out-gassed sample in the reactor, it was purged with 150 NmL/min of N_2 for 40 mins to drive out any air in the system and create a N_2 rich environment before beginning adsorption.

Adsorption: The adsorption step was started by feeding 100 NmL/min of the gas mixture (15 % v/v CO_2 in N_2) dry, or wetted with 15 % RH, at room temperature (approximately 23 °C) and 1 bar. The working capacity presented in sections 3.1 as well as capture capacity and breakthrough plots presented 3.5.1 were obtained from this step. The CO_2 concentration in the effluent gas was continuously monitored as a function of time until it reached the CO_2 concentration at the inlet, i.e., until saturation was reached (breakthrough curve experiments) or for fixed pre-set adsorption time for cycles without adsorbent saturation (breakthrough was avoided).

Regeneration: The CO_2 was desorbed by switching the gas flowrate to 20 NmL/min of N_2 and raising the temperature to 100 °C (+/-3 °C). For both TSA and MWSA cycles 60 mL reactor holding the same quantity of sample (6 g), which is volumetrically equivalent to 12.50 cm^3 of Norit R and 9.8 cm^3 of 13X, was mounted inside the microwave cavity. The power and the pre-set temperature were monitored and controlled during regeneration using procedure described in section 2.2 for both heating systems. For unsaturated cycles, heating was terminated after 7 mins for Norit R and after 10 mins for 13X. These heating times were selected based on series of tests performed to find out the minimum microwave heating period that allows over 90 % removal of the adsorbate on a dry basis.

Finally, the method employed for the quantitative determination of the amount of CO_2 adsorbed and desorbed is reported in detail in our previous work [19].

2.3.2. Moisture control in the feed gas for wet cycles

A key challenge in implementing a cyclic adsorption-based process for cleaning a gaseous stream such as flue gas is obtaining specific insight into the interaction between the adsorbent material and each of the different gas phase components in the stream. In the case of flue gas, an effective CO_2 capture can be achieved if other components in the stream have minimum negative interference with the selectivity and capture capacity of the adsorbent for carbon dioxide. In that regard, experiments were devised to wet the impurities-free or pre-cleaned flue gas (add moisture) and investigate the effect of moisture in the conventional and microwave-assisted carbon capture processes.

For controlling the moisture addition in the system, a side-line (bypass) was diverted from the main gas line (carrying dry gas) and connected to a conical flask containing water, then re-joined with the dry gas line just before it passes through the humidity sensor. The sensor is housed in a stainless-steel casing with 1/8-inch tube fittings on either side to permit an online connection to the gas line. When running wet experiments, a portion of the gas flows through the side-line, passing over the water in the flask, collecting moisture, then joining the dry gas at a T-junction. The wet gas mixed with dry gas passes over the humidity sensor. The portion of the gas that went over the water is 100 % saturated before mixing with the dry gas. After the mixing, the humidity level that is reduced and recorded by the humidity sensor. The moisture level in the final gas is adjusted by controlling the amount of gas that passes through the wet line. This is achieved by adjusting the position of the needle valve which is placed after the T-junction where the wet line and the dry lines split. Finally, the humidity sensor signal is converted from electric potential (V) to relative humidity (%) using manufacturer pre-determined calibration curves (which consider the temperature) [20].

3. Results and discussions

3.1. Effect of humidity and regeneration method on working capacity and regeneration extent

Considering that typical flue gas from coal-fired combustion processes contains around 15 % v/v of moisture, experiments were designed to assess the impact of humidity on the working capacity and

regeneration extent (CO_2 desorbed percentage) in both regeneration methods. The experimental results obtained are presented in Table 1 below.

Table 1. CO_2 desorbed with microwave (MWSA) and conventional (TSA) heating. Adsorption step feeding gas: dry (15 % v/v CO_2 in N_2) and wet (15 % v/v CO_2 in N_2 + 15 % RH)

Adsorbent	**Heating mode**	**Working capacity (mg/g)**		**Desorbed percentage (%)** *	
		Dry gas	Wet gas	Dry gas	Wet gas
Norit R	MWSA	20.69 ± 0.35	24.08 ± 0.94	100.00 ± 1.70	96.00 ± 3.74
	TSA	18.92 ± 0.00	17.24 ± 0.51	100.00 ± 1.89	81.67 ± 2.49
13X	MWSA	76.75 ± 5.74	64.39 ± 1.95	82.00 ± 7.12	90.00 ± 3.56
	TSA	63.75 ± 4.51	51.83 ± 4.19	76.67 ± 6.94	76.67 ± 7.72

Numerical values are provided with the ± Standard Deviations (SD)

* Desorbed/regenerated (%) with respect to the total amount adsorbed in the adsorption step, this is the base for all regeneration calculations

Wet gas total flow rate: 100 Nml/min

Table 1 displays the CO_2 working capacity (defined as the difference between the amount captured under adsorption condition and that retained under desorption conditions [21]) and CO_2 desorbed (in percentage) of Norit R and 13X, values averaged from three short cycles (unsaturated samples as adsorption step was stopped before breakthrough). The short cycles were designed based on breakthrough time (t_b, measured at $C/C_o \leq 0.05$) obtained from a previous run with saturation (t_b was approximately 5.3 mins for both Norit R and 15 mins for 13X under the same experimental conditions corrected with the blank experiment to subtract the delay time due to the void space in the system). Results are compared for wet versus dry flue gas within one regeneration method (i.e. either MWSA or TSA) as well as one regeneration strategy against the other for each gas condition (i.e. MWSA vs TSA).

Before discussing the results presented in Table 1, there are two observations from the data which need to be clarified. Firstly, the occurrence of working capacity in cycle 1 is not showing much difference from cycles 2 and 3 in any adsorbent for the same heating mode and same gas conditions. In a typical cyclic swing operation, the first run yields a high capacity because the adsorbent is fresh. This run is normally not considered in a realistic, practical operation; therefore, only the working capacities of

subsequent cycles are counted. To account for this, the samples were first exposed to a cycle of full adsorbent saturation followed by full regeneration in both TSA and MWSA. Only then were these short unsaturated cycles started. Hence, cycle 1, in this case, corresponds to the working capacity of a previously regenerated sample, and not a fresh one. This is the reason why the working capacity of cycle 1 is fairly similar to cycles 2 and 3. The second observation is that cycle 1 in MWSA is always higher than that in TSA, for the two adsorbents in both gas conditions (dry and wet). This is because microwave heating regenerated the adsorbents more extensively compared to TSA during the full regeneration after the initial full saturation of the fresh sample. This led to higher working capacity in cycle 1 which is maintained in subsequent cycles (2 and 3) in MWSA.

As can be seen in Table 1, for Norit R under MWSA, the addition of moisture to the gas mixture increased the CO_2 working capacity from 20.69 to 24.08 mg/g, corresponding to the 16.38 % rise. In the case of samples regenerated with TSA, the working capacity decreased by 11.63 % (i.e. from 18.92 to 17.24 mg/g). Comparing MWSA with TSA for Norit R, samples regenerated with microwave heating maintain a higher working capacity than those regenerated with conventional heating in both dry and wet conditions. The improvement in working capacity due to the presence of moisture is maintained in MWSA since full regeneration is attained between cycles. With TSA on the other hand, the working capacity is hindered by the lack of full regeneration in cycles. Regarding the CO_2 desorbed percentage for Norit R, in the dry case, samples achieved full regeneration (100 %) in both MWSA and TSA. In the wet case, regeneration dropped to 81.67 ± 2.49 % in TSA, whereas in MWSA full regeneration was fairly achieved (96 ± 3.74 %).

For 13X, CO_2 working capacity is lower under wet gas conditions regardless of the regeneration strategy. With MWSA, the working capacity reduced from 76.75 mg/g in dry conditions to 64.39 mg/g in wet conditions. With TSA, it was reduced from 63.75 to 51.83 mg/g in the same order. These are significant reductions, equivalent to 16.1 % and 18.7 % for MWSA and TSA, respectively.

Additionally, comparing MWSA and TSA for the dry gas, the working capacity is substantially higher under MWSA (by 16.94 %). Considering the same comparison in the wet gas, again the working capacity is 19.50 % higher in MWSA than TSA which is a considerable increase. The greatly enhanced

working capacity observed in MWSA for the two gas conditions tested is a result of a superior adsorbent regeneration achieved with microwave heating over conventional heating.

The effect of the presence of moisture on the enhancement of CO_2 adsorption capacity with activated carbons has been previously reported [22]. Both positive and negative impact of moisture on CO_2 adsorption have been seen. Normally, at sub-atmospheric pressures, negative impact is reported where at higher pressures, a positive impact is confirmed [23]. Using a commercial activated carbon (Norit R) and two biomass driven activated carbon, Duran *et al.* found that the presence of 16 % RH significantly reduced the CO_2 uptake [24]. Although there are some reports which claim that presence of humidity has no effect on the CO_2 adsorption regardless of the moisture level, others indicate that when the adsorption duration is prolonged, the water eventually displaces part of the initially adsorbed CO_2 leading to smaller capture capacity [23]. Sun *et al.* who measured CO_2 uptake at 2 ºC found that at low pressures the CO_2 uptake was reduced in the presence of moisture compared to dry case, however when the pressure was set at 15-20 bar, the capacity increased substantially. They attributed it to the formation of CO_2 hydrate [25]. Similarly, Jalilov *et al.* who used asphalt derived AC (uGil) found a drastic increase of CO_2 uptake from 15 to 48 mmol/g at 20 bar and -15 ºC when adsorbent was pre-hydrated compared to dry condition [26].

Nonetheless, as water is highly dielectric, its presence might have assisted the microwave regeneration with an elevated microwave absorbance. Even so, the hydrophobicity and the faster CO_2 adsorption kinetics could help lessen competition to the adsorption of water, it does not necessarily explain the boosted performance on working capacity observed by the activated carbon with the wet gas condition. This unusual moisture-enhanced CO_2 adsorption capacity was observed by Chen *et al.* who worked on two metal−organic frameworks (MOFs), PCN-250(Fe_3) and PCN-250(Fe_2Co) [27]. With 50 % relative humidity, CO_2 adsorption capacity increased by 54.2 and 68.9 % respectively compared to the dry gas conditions. In an attempt to explain the underlying reason, the group has suggested a possible adsorption mechanism. They report the adsorbed water acts as a directing agent for enhanced CO_2 adsorption through confinement effect, meaning water molecules restrict the pore openings to metal sites, therefore pushing CO_2 molecules closer into adsorption sites and promoting increased interaction.

Similar reasoning can also be applied here to elucidate what was observed in this work. As reported by Rodríguez-Mirasol *et al.* [22] and Xu *et al.* [28, 29], primary adsorption of water on activated carbons arises from hydrophilic surface sites with functional groups. When such sites occur in abundance, neighbouring adsorbed water molecules form hydrogen bonding between them which gives rise to cluster formation. This leads to micropore filling as well as migration to meso- and macro-pores through condensation. In such instances, moisture presence affects adsorption capacity for CO_2 and other species negatively. From the increased capture capacity in wet tests, it seems that the available hydrophilic sites on Norit R are not significant enough to adsorb moisture that can foster cluster formation, however, a sufficient amount of water moisture was adsorbed, which resulted in an adequate confinement effect. Any adsorption sites lost due to competition from the water were possibly outweighed by the positive impact from the confinement effect which forces the CO_2 to interact and stay longer inside the channels and openings where pore dimensions are reduced by the water molecules.

In the case of 13X, the impact of water on CO_2 adsorption is always negative and quite severe in most cases. The influence of water on the CO_2 adsorption is different for the two adsorbent types, regardless of the amount adsorbed [23]. Unlike the Norit R, 13X is highly hydrophilic and on that account, the existence of moisture is expected to bring competition for adsorption sites resulting in decreased CO_2 uptake. The obtained results confirm what was anticipated. Applying a similar concept of what was said about the ACs, the impact of moisture on 13X can be explained too. Inside the structure of 13X there are sodium cations (Na^+) for balancing the negatively charged framework due to the Si-O-Al. Polar water molecules can couple with either of them. In addition to that, silanol functional groups are known to exist on the surface of 13X, which can hydrogen bond with moisture [30]. A combined effect of the charged framework and the surface silanols seem to raise the amount of water adsorbed to cluster formation level, hence, the observed reduction in adsorption capacity in the wet cases compared to the dry cases in both MWSA and TSA. The decrease in uptake capacity in 13X can also be linked to its textural properties. 13X has more than two times smaller average micropore width (0.46 nm) than the activated carbon Norit R (0.94 nm). CO_2 and H_2O have a combined kinetic diameter of 0.595 nm (CO_2 at 0.33 nm and H_2O at 0.265 nm). This suggests water can block the micropore channels for CO_2 in

13X, as there will be not enough space around the adsorbed water molecule for the CO_2 as their combined diameter will be bigger than the channel (pore) diameter. This means it will not get access to the adsorption sites beyond the point where water is adsorbed. The effect of pore blockage by the water in the activated carbon is minimal since, in most of the pores, there will be sufficient space left for the CO_2 to pass through.

To summarise, Norit R exhibits the best working capacity under the wet gas conditions with MWSA and performs poorest under the wet condition but with TSA. Contrary to the AC, moisture presence is unhelpful for working capacity in 13X. It performed the best in the dry gas conditions and with MWSA, whereas the wet conditions under TSA yield the poorest result. The superior performance with MWSA seen in both adsorbents in each gas condition is due to better regeneration realised under MWSA compared to TSA, which indicates the great potential this technology has on the regeneration of CO_2 loaded sorbents.

3.2. CO_2 Productivity, Purity, and Recovery

Productivity, purity, and recovery are key performance indicators. Any cyclic adsorption-desorption process should be designed with these parameters in mind by optimising the swing adsorption process in a way that delivers an acceptable level of each of them. Purity, in this context, refers to the optimal level of the extract (targeted adsorbate) in the exit line, subject to a pre-specified standard for the process. It gives an indication of the adsorbent selectivity towards the target component, CO_2 in this case. The recovery parameter indicates the suitability of the adsorbent as a capturing agent for the target adsorbate as well as the suitability of the selected regeneration method. Evaluating the productivity parameter helps in deciding whether it is economically worthwhile to run the process or not, by relating the amount captured per cycle to the total process time and amount of adsorbent. It is an important criterion in designing adsorption systems especially in temperature swing adsorption, where cycle time is normally high due to longer heating and cooling times involved. The ultimate goal is to obtain high productivity without compromising the level of purity and recovery set.

In separating the post-combustion flue gases from coal/natural gas-fired power plants, the raffinate and the extract (targeted adsorbate) are N_2 and CO_2, respectively. CO_2 productivity, purity, and recovery are discussed and compared for the two heating sources (microwave and conventional heating) in this section, as evaluating these three parameters help in assessing the performance of each of the swing adsorption processes (MWSA and TSA).

Productivity is defined as the amount of CO_2 captured per adsorbent unit mass and time. Productivity was calculated for each cycle, for which cycle time is the total time considering the adsorption and regeneration steps. The time period accounted as cycle time from the regeneration step was taken as the time required to regenerate 99 % of the CO_2 previously captured, starting from the moment heating is commenced in the regeneration step. This way, most of the prolonged period encountered at the tail of desorption profiles is avoided, should cycle time were to be based on 100 % regeneration. Productivity was calculated by using the following equation:

$$\text{Productivity}\left(\frac{\text{mol}}{\text{kg}\cdot\text{h}}\right) = \frac{\text{Qad}_{CO_2}}{(\text{m})\cdot(\text{t})} \qquad \text{(Eq. 6)}$$

where Qad_{CO2} (mg) is the CO_2 adsorbed during the adsorption step, m is the adsorbent mass (g) and t (h) is the cycle time.

The purity of the CO_2 recovered downstream the adsorber during the regeneration step is defined as the amount of CO_2 in the adsorber's outlet per total gases (i.e. CO_2 and N_2) and was determined using Equation 7. It is worth saying that the purge gas (N_2) fed into the system during regeneration is excluded in evaluating the purity. However, the co-adsorbed N_2 during the adsorption step, which is coming off with the CO_2 during heating, is added in the calculation,

$$\text{Purity}\ (\%) = \frac{\text{Qde}_{CO_2}}{\text{Qde}_{CO_2} + \text{Qde}_{N_2}}\cdot(100) \qquad \text{(Eq. 7)}$$

where Qde_{CO2} and Qde_{N2} (mg) are the CO_2 and N_2 desorbed respectively.

Recovery is evaluated to determine the percentage of CO_2 captured compared to the amount of CO_2 fed. It is defined as the amount of CO_2 in the product per total amount of CO_2 in the feed. The recovery was calculated using Equation 8:

$$\text{Recovery } (\%) = \frac{\text{Qde}_{CO_2}}{\text{Q feed}_{CO_2}} \cdot (100) \qquad \text{(Eq. 8)}$$

where $Qfeed_{CO2}$ (mg) is the total CO_2 fed during the adsorption step.

Figure 2 presents purity, recovery, and productivity obtained with MWSA and TSA, for a 6 g sample of Norit R, and 13X. Overall, both samples presented higher CO_2 recovery with MWSA compared to TSA. Recovery also shows the highest variations of the three parameters evaluated, between adsorbents, heating modes, and cycles. For Norit R, the average recovery found is 96.1 % in MWSA compared to 75.1 % in TSA. This is due to lower regeneration achieved under TSA which resulted in a lower amount desorbed as well as lower capture capacity in subsequent cycles. For 13X, recovery is on average 15 % higher with MWSA (87 %) compared to TSA (72 %). In this case, the amount recovered is the lowest in cycle 1 at 83.3 and 64.2 % in MWSA and TSA, respectively. This implies that a large portion of the CO_2 fed into the system is not recovered. This could be due to a lack of full regeneration where a large proportion of the gas remains in the material. Results from own measurements indicate that 13X has a much higher average isosteric heat of adsorption (Q_{st}), 49.94 kJ/mol, compared to the activated carbon at 25.15 kJ/mol. Q_{st} gives an indication of how much energy (e.g. kJ) must be provided to release the adsorbate (mol of CO_2) from the respective adsorbents. It is then interpreted that the regeneration temperature selected in this case (13X) was not enough to provide all the energy needed. Hence, a substantial amount of the pre-adsorbed CO_2 was not released from the zeolite, especially when conventional heating was applied. Although full regeneration was neither achieved in the case of MWSA, the CO_2 recovery was greatly higher when unconventional heating was applied.

Both samples show stable average purity of over 98 % (Figure 2 b). For Norit R, average purities of 99.6 % with MWSA and 98.4 % with TSA were obtained. The average purity for 13X is stable at 99.4 % in both cyclic separation processes. Productivity was found stable for each heating mode, but higher in MWSA for both samples compared to TSA. Average productivity for Norit R is 25 % higher in MWSA

compared to TSA (814.29 and 612.77 mol/(kg h), in the same order). Average productivity in 13X is 27 % higher in MWSA than in TSA (1654.24 and 1200.00 mol/(kg h), in the same order). The reasons are that capture capacity was higher and cycle time was shorter in the MWSA process, both of which favour improved productivity.

Except for recovery, where there are variations among cycles, the other two parameters (purity and recovery) are stable within three cycles for the same heating source. The observed difference in the recovery is because the CO_2 feed is constant for all cycles where the amount coming off is different from cycle to cycle which resulted in a changing numerator and a constant denominator in the relevant equation, hence variations. The stability seen in the productivity is due to the amount captured being very close between cycles, which indicates that regeneration achieved in each cycle was stable and thus, reproducible. Purity is also both high and stable because the amount of N_2 co-adsorbed with the CO_2 is very small and does not vary much from cycle to cycle.

In conclusion, higher performance is achieved under MWSA for each of the three parameters investigated in this section: productivity, purity, and recovery, in both adsorbents, tested. High and stable purity is obtained in both samples and highest productivity is shown by 13X with MWSA. Recovery however presented greater variations than purity and was the lowest for 13X with TSA. Zeolite 13X performed better than the activated carbon in productivity terms both in MWSA and TSA.

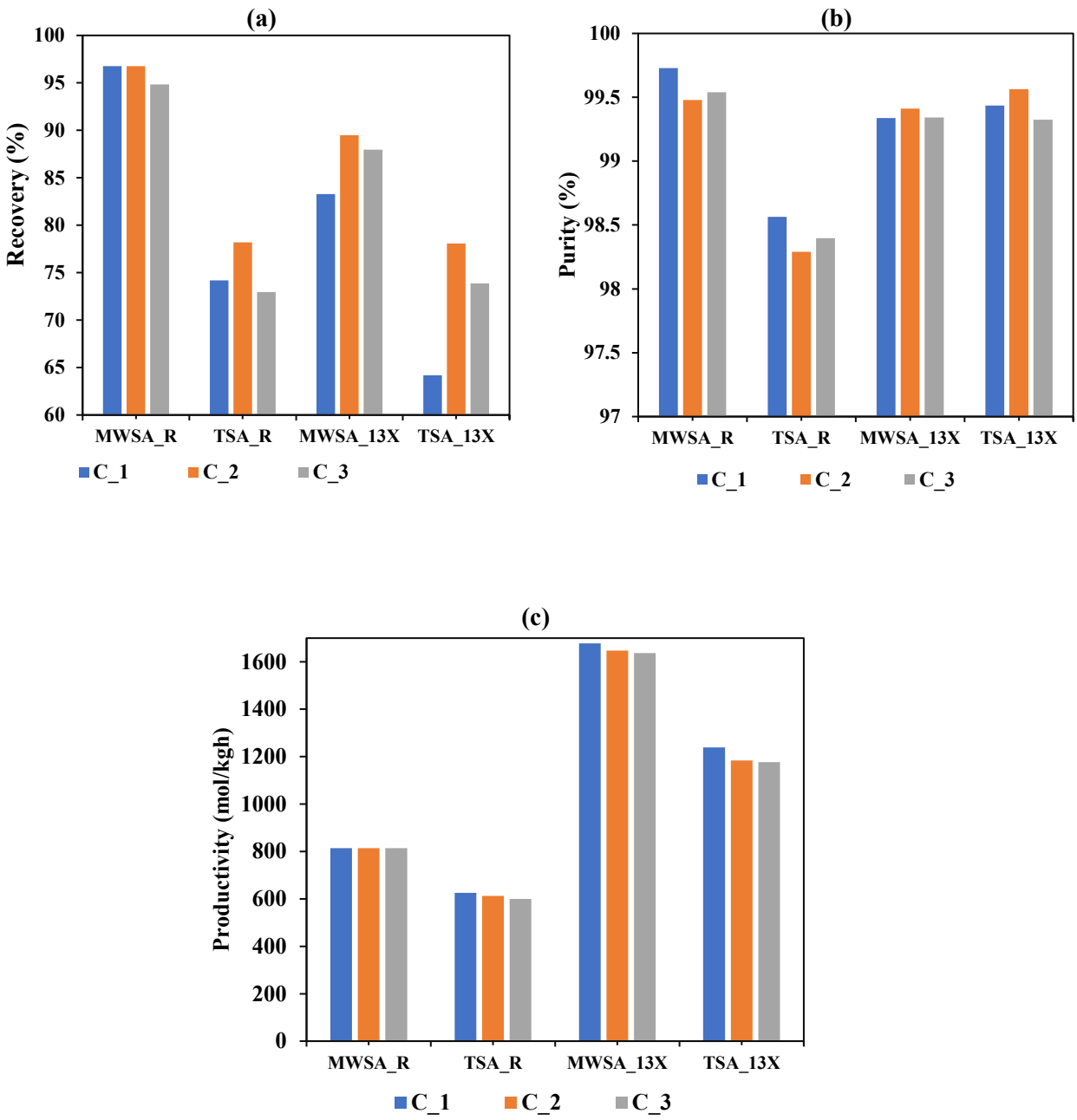

Figure 2. CO_2 Recovery (a), Purity (b), and Productivity (c) of Norit R and 13X for 6 g sample in MWSA and TSA with three short cycles. C_1, C_2 and C_3 stand for cycle 1, cycle 2 and cycle 3 respectively.

3.3. Extent of CO_2 regeneration

The fraction of adsorbate removed with respect to the total regenerated at a given time is evaluated for both heating methods. This gives an indication of the regeneration time needed to achieve a determined percentage of regeneration for each adsorbent and heating method. From this, a comparison between MWSA and TSA can be made throughout the whole regeneration period as well as at specific

regeneration levels of interest. For instance, to compare how much is the regeneration time needed to achieve 50, 80, 90, or 99 % regeneration.

To distinguish between heating time and regeneration time in this context, the two terms are defined as follows:

- *Heating time:* the period when heating power is on.
- *Regeneration time:* heating time plus the period needed to get the CO_2 concentration in the exit line to 0 % v/v while sweeping with N_2.

Table 2 summarises the time needed to remove 50, 80, 90, and 99 % of CO_2 from each adsorbent (6 g) with MWSA and TSA. Every regeneration time needed to achieve such regeneration percentages was smaller under microwave-assisted swing for both adsorbents. Despite 13X having shorter regeneration times in MWSA, the difference is up to 90 % regeneration is small (1 min), compared to Norit R. However, for 99 % regeneration, the difference in regeneration time between the MWSA and TSA is larger with 13X (18 mins) as opposed to Norit R (5 mins). This dissimilarity is most likely rooted in differences in their properties (e.g. dielectric properties, textural properties, and packaging properties (bulk density, bed height, void space, length/diameter ratio)). At the desorption temperature used in these experiments (100 °C), 13X has a lower dielectric constant (ε') and higher loss factor (ε'') than Norit R (ε': 3.64 vs 15.36, and ε'': 0.92 vs 0.05, for 13X and Norit R respectively. Quoted values were measured for these adsorbents. This implies lower microwave absorbance but higher heat dissipation in 13X compared to Norit R. However, that was not observed from the temperature rise recorded during microwave heating. This could indicate that the higher microwave absorbing ability of the activated carbon is more beneficial than the higher heat dissipation ability of the zeolite at the lower regeneration temperature employed in these tests. It could also be speculated as the microwave power level used in this work to be below the threshold required by the zeolite to cause a quick temperature increase. 13X also has a higher pressure drop (0.0034) in the bed compared to Norit R (0.0025) which had a restricting effect on the flow of the gas released as well as the sweeping gas, hence the longer regeneration times.

For Norit R, 17, 22, 25, and 39 mins were needed with MWSA and 21, 27, 32, and 44 mins with TSA to achieve 50, 80, 90, and 99 % of CO_2 regenerated, respectively. The times needed to regenerate from

90 to 99 % were 14 and 12 mins in MWSA and TSA, respectively. That is equivalent to 36 and 27 % of the total regeneration time, in that order.

For 13X, the time needed to achieve the same regeneration percentage of up to 90 % for each of the two heating modes is 1 min smaller with MWSA compared to TSA. However, in this case, the time needed to achieve 99 % was 18 mins longer with conventional heating. Noting from the time gap between t_{90} and t_{99}, it indicates that removing the last 9 % of the adsorbate remaining on the zeolite is the most time (and energy) consuming part of the regeneration process. In fact, half of the regeneration time was spent in removing the last 9 % of CO_2 (i.e. from 90 to 99 %) in TSA. With microwave heating, on the other hand, the required time for removing the last 9 % was a third of the total regeneration time. This suggests that regenerating these adsorbents to 90 % rather than to 99 % would dramatically reduce regeneration time and energy consumed during regeneration, which in turn will improve productivity greatly. This is the basis for running cycles with unsaturated adsorbents that are not fully regenerated. The working capacity, which is smaller than the full capture capacity, might be the compromise to take in this separation process, however, the advantages gained from the reduced energy applied as well as enhancement in the productivity due to the reduced regeneration time are larger (i.e. 34 and 71 % increase in productivity for MWSA and TSA respectively).

Table 2. Time needed to achieve 50, 80, 90, and 99 % regeneration with TSA and MWSA

Adsorbents	**Heating method**	**t_{50}**	**t_{80}**	**t_{90}**	**t_{99}**
Norit R	MWSA	17	22	25	39
	TSA	21	27	32	44
13X	MWSA	19	26	31	46
	TSA	20	27	32	64

t_{50}, t_{80}, t_{90} and t_{99} = time (in min) at which the regeneration percentage achieved is 50, 80, 90 and 99 %

3.4. Desorption kinetics

Kinetic studies provide a way of predicting the desorption behaviour of adsorbate from a given adsorbent in specified operating conditions (i.e. temperature, pressure, feed composition, etc). They help obtain an understanding of the intrinsic interaction and mechanisms between the adsorbate species and the surface of the solid. One could evaluate important process parameters including desorption rate

and desorption extent from such kinetic studies, and from that, could forecast how they change with different process conditions using models. In this regard, the regeneration data were fitted to three kinetic models and to assess the process of CO_2 desorption from the adsorbents. In this work, the three models of Pseudo-first order model (PFO), Pseudo-second order model (2^{nd} order), and Avrami's model are selected. Their applicability in predicting the regeneration process is evaluated and results are presented in this section.

3.4.1. Pseudo-first order model (PFO)

The PFO is conventionally applied to the adsorption stage with the assumption that adsorption is proportional to the number of vacant sites available on the solid for the adsorbate [31]. Since desorption is the reverse process, the model can be indirectly applied, in this case assuming that number of vacated sites are proportional to the desorbed amount during regeneration. The linear form of PFO is shown in Eq. 9 below [32]:

$$\ln\left(q_e - q_t\right) = \ln q_e - kt \qquad \text{(Eq. 9)}$$

In the case of desorption, q_e is the total amount of CO_2 desorbed at end of the regeneration process (mg), q_t is the amount of CO_2 desorbed (mg) at time t (min), and k is the desorption rate constant (min^{-1}).

A plot of ln (q_e-q_t) *vs* t gives a straight line whose slope is rate constant (k) and the intercept is ln q_e. The goodness-of-fit (R^2) value closer to unity is an indication that the PFO model fits the experimental data and is suitable for predicting the desorption process.

3.4.1 Pseudo-second order model (2^{nd} order)

The Pseudo-second-order model represents an adsorption process where the rate is declining fast with time as adsorption sites decrease over time as they are being occupied. In general, four different pseudo-second-order model expressions exist in the literature for determining adsorption kinetics. The expression selected in this work was originally proposed by Ho and McKay [33], as the agreement between the adsorption data and the model predictions was found to be high [34]. One of the major assumptions regarding adsorption kinetics in the pseudo 2^{nd} order is that the bulk concentration of the

solute (adsorbate) stays fairly constant over time. A similar assumption is also ingrained in the PFO [34].

The linear form of the Pseudo-second-order model used is presented in Eq. 10 as follow:

$$q_t = \frac{k_2 qe^2 t}{1 + k_2 qe^2 t} \quad \text{(Eq. 10)}$$

where k_2 is the kinetic rate constant, q_e is the amount of CO_2 adsorbed at equilibrium (mg), q_t is the amount of CO_2 adsorbed (mg) at time t (min).

A plot of t/q_t *vs* t gives a straight line with slope and intercept. q_e and rate constant (k_2) can be calculated from it as, q_e = 1/slope and k_2 = slope^2/intercept.

3.4.2 Avrami's Model

Whilst Avrami's fractional-order kinetic model is formally developed to simulate phase transition and crystal growth of materials, some researchers have applied it to describe the kinetics of CO_2 adsorption/desorption with adsorbents, especially amine-modified silica and carbon nanotubes. In the adsorption process, the integrated form of the models is described by the following equation [35, 36]:

$$q_t = q_e(1 - \exp(-kt^n)) \quad \text{(Eq. 11)}$$

where k is the Avrami kinetic constant (min^{-1}), n is the Avrami exponent, q_e is the amount of CO_2 adsorbed at equilibrium (mg), and q_t is the CO_2 adsorbed amount at time t (min). The Avrami's exponent (n) value is generally between 0 and 4. It indicates the direction of growth from the adsorption sites. For n = 4, it is three-dimensional, for n= 3 is two-dimensional growth, and n= 2 is for one-dimensional growth. On homogeneous surfaces where the possibility of adsorption is equal anywhere, n = 1 [37].

In applying the model to the desorption process, Eq. 11 is transformed into the following expression [36]:

$$y = 1 - \exp(-kt^n) \quad \text{(Eq. 12)}$$

where y is the desorption proportion which is defined as the ratio of mass loss (mg) at time t (min) to the total mass loss (mg) at the end of the desorption process.

From Equations 9, 10, and 12, the CO_2 desorption proportion (ratio of CO_2 amount desorbed at time *t* to the total amount desorbed) was evaluated for MWSA and TSA for the adsorbents, Norit R and 13X. The data obtained from the three models are compared to the experimental results and plotted together in Figure 3.

Overall, Avrami's model showed the best fit to the experimental data for both adsorbents in both heating modes. On the other hand, neither the PFO nor the pseudo 2nd order presented a good fit as their predictions were off either by overestimating or underestimating most parts of the data.

For Norit R, the PFO overestimated the CO_2 desorbed proportion in the first 16 and 23 mins in MWSA and TSA, respectively. It then fallen slightly below the experimental data, but the overall prediction was in close agreement with experimental data in the plateau region. For 13X, the PFO overestimated the first 14 mins in both MWSA and TSA, however, this overestimation is not as large as that seen in the Norit R sample. Nonetheless, the CO_2 desorption proportion from 13X was widely underestimated by PFO for the rest of the regeneration up until near completion.

The pseudo 2nd order, which showed the worst fit, out of the three models broadly, overestimated or underestimated in both adsorbents in both heating modes. The difference between adsorbents is the time at which the predicted curves cross the experimental curves and at what CO_2 desorption proportion. For Norit R, the model curves cross the experimental curves at 16 mins and 18 mins with 87 and 77 % desorption proportion for MWSA and TSA respectively. For 13X, pseudo 2nd order overestimated up until 75 % desorption at 16 mins for MWSA and 85 % desorption at 21 mins for TSA. After that, the model underestimates, with a fairly wide gap between the predicted points and the experimental points, especially for MWSA.

As described above, both the PFO and the pseudo 2nd order assume bulk adsorbate concentration that is not changing with process time. In desorption terms, this cannot be true. In the desorption process of a dynamic system, the concentration of the adsorbate is low at the beginning, then as heating is started and the adsorbate is being released, its concentration increases in the bulk. This is followed by a decrease in the later stages of the process as most of the adsorbate is released from the sites and removed

from the system with the sweeping gas. If not the only one, this could most certainly be one of the reasons why these two models, the PFO and the pseudo 2nd order, are not good fits for these experimental data.

Both adsorbents show overall goodness-of-fit (R^2) values above 0.86 for the PFO as presented in Table 3. In the 2nd order, the goodness of fit for Norit R is fairly low (0.54 in MWSA and 0.51 in TSA) which is in line with the graphical observation in Figure 3 a. For 13X, however, it shows a fairly high value of goodness-of-fit (0.82). This does not match with the observed graphically, a similar situation that is found with PFO, which indicates that R^2 may not be the most suitable regression analysis for this particular application.

On the other hand, both adsorbents show excellent goodness of fit (0.99) in Avrami's model, supported by perfect alignments of experimental and predicted data points throughout the entire time range. A very minor exception to that is the first 3-5 mins where the model points fall below experimental values, especially in the Norit R sample. The values of Avrami's exponent (*n*) obtained in these analyses are tabulated in Table 5an and as observed from Table 5, all values are between 1 and 2 for both adsorbents in both microwave and conventional regeneration. This suggests one-dimensional growth. In the context of CO_2 desorption, this could mean that the desorbed CO_2 gas formed a multi-layer during the adsorption step, which is in agreement with the Brunauer–Emmett–Teller (BET) adsorption mechanism's theory.

As presented in Figure 3, Avrami's model adequately predicted the desorption proportion of CO_2 as a function of time, signifying the applicability of the model to the CO_2 desorption process mechanism in these adsorbents. Considering its practical relevance, for example, one could study different desorption process conditions (temperature, pressure flow rate, etc) and compare changes in certain factors such as the rate constant k, the Avrami's exponent (n), and desorption profiles, making it possible to obtain correlations that can be used to predict the desorption profiles and mechanisms for a variety of process conditions without experimentations, for instance with the use of a simulation.

Table 3. Pseudo-first-order (PFO) model fitting parameters

Pseudo-first-order				
	Rate constant (k), min^{-1}		**R^2**	
	MWSA	TSA	MWSA	TSA
Norit R	0.085	0.100	0.94	0.87
13X	0.077	0.072	0.98	0.98

Table 4. Pseudo-second-order model fitting parameters

Pseudo-second-order				
	Rate constant (k_2), g mg^{-1} min^{-1}		**R^2**	
	MWSA	TSA	MWSA	TSA
Norit R	0.0011	0.0004	0.54	0.51
13X	0.0002	0.0004	0.82	0.82

Table 5. Avrami's model fitting parameters

Avrami's model						
	Rate constant (k), min^{-1}		**Avrami's exponent (n)**		**R^2**	
	MWSA	TSA	MWSA	TSA	MWSA	TSA
Norit R	0.034	0.008	1.4	1.8	0.99	0.99
13X	0.032	0.025	1.4	1.4	0.99	0.99

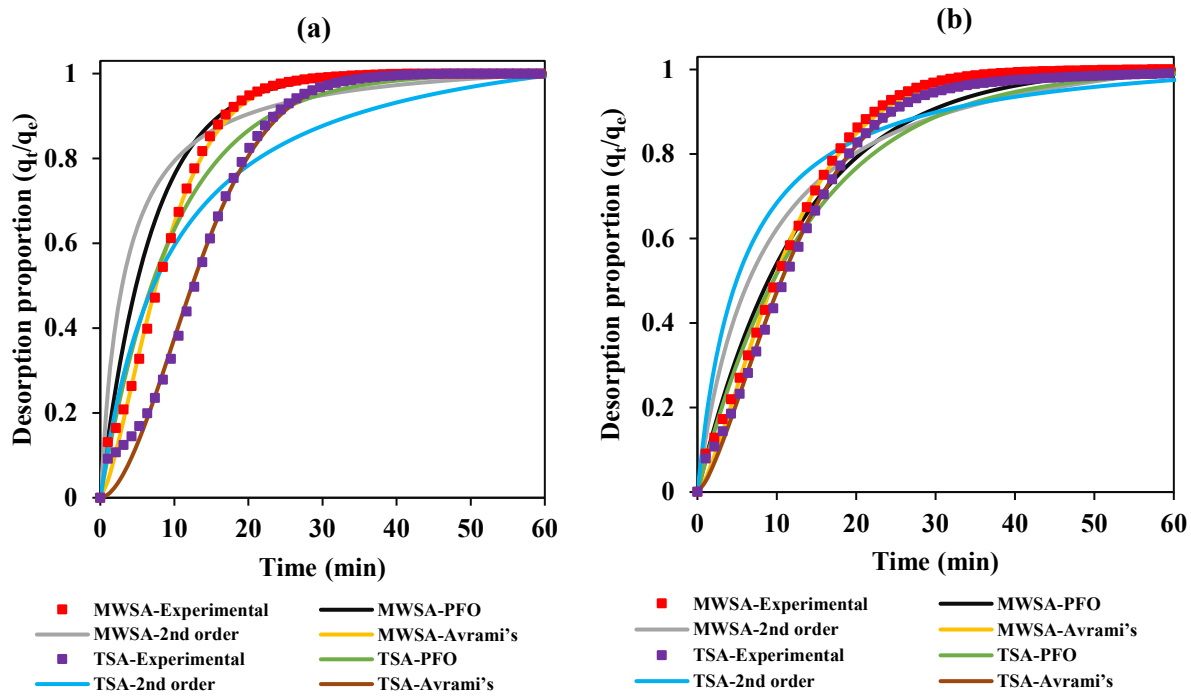

Figure 3. Experimental and modeled CO_2 desorption proportion curves (ratio of amount of CO_2 desorbed at any time with respect to the total amount desorbed) of Norit R (a) and 13X (b) for MWSA and TSA. Unsaturated samples in the adsorption step under wet flue gas. Sample weight: 6 g.

3.5. Effect of sample size on dynamic MWSA and TSA separation. A comparative analysis

3.5.1 Effect of the sample size on CO_2 adsorption/desorption profiles, and the maximum uptake capacity. MWSA *vs* TSA

Acknowledging that microwave heating is volumetric and that the heating efficiency of a determined microwave cavity would be increased if the quantity of material to be heated is enlarged, further experiments were performed with Norit R with the mass of the sample increased by 8 times (i.e. from 6 to 48g) for the wet condition in both MWSA and TSA. To keep the total process within a reasonable time, the feed gas flow rates in the adsorption and regeneration steps were increased by 4 times, from 100 to 400 Nml/min and from 20 to 80 Nml/min, for the adsorption and regeneration steps, respectively. Feeding gas flow rates were optimised experimentally to accommodate the increase of column volume due to the increased adsorbent mass. The selected flow rates allowed for well-defined breakthrough and desorption curves to be obtained, as gas residence time was sufficient for the adsorption and

regeneration to occur. Higher flow rates, however, impacted the breakthrough time and were found detrimental to the CO_2 uptake capacity due to the reduction of the contact time between the adsorbent and adsorbate. The CO_2 uptake capacity for experiments with saturated and unsaturated adsorbents is shown in Table 6 for both sample masses.

Table 6. CO_2 uptake capacity of Norit R, with and without saturation. Sample mass: 6 and 48 g (adsorption gas feeding flow rates: 100 and 400 Nml/min, respectively)

CO_2 uptake capacity (mg/g)		
	Sample mass = 48g	Sample mass = 6g
Saturated	37.40	37.40
Unsaturated	16.28	25.08

Figure 4 displays the CO_2 breakthrough curves measured with Norit R. It can be observed that the breakthrough time increased with the increase in sample size (7.43 min for the 6 g and 14.85 min for the 48 g, respectively). This confirms that it takes a longer time for the CO_2 to travel through the increased bed volume, delaying its detection downstream the reactor after saturation. However, it does not indicate an increased capture capacity, as the total amount of CO_2 retained in the bed is normalised by the sample size to calculate the uptake capacity. In the unsaturated case, a capacity of 16.28 mg/g is recorded for the large mass which is a 35.1 % drop compared to 25.08 mg/g obtained with the smaller mass. It is worth noting that this reduction in capacity was not observed in the saturated case of the large sample. However, although the uptake at saturation was not affected by an increase in sample mass, the process required a longer time to achieve full saturation. The less pronounced slope of the curve after the breakthrough point for the large sample indicates the reason for the drop, that is, the increase in width in the mass transfer zone (MTZ) in the larger sample. It then means that the CO_2 which forms the front of the MTZ moves quicker to the reactor outlet, resulting in a fast-moving MTZ front. This led to the creation of an MTZ that is spread over a large area of the bed where active adsorption is taking place much later than the time the CO_2 is detected in the micro-GC (i.e. breakthrough point reached). The bed saturates slowly for an MTZ with a fast-moving front, which is

suggested by the smoother slope compared to the curves observed with the smaller sample. Contrarily, it saturates fast for an MTZ with a slow-moving front relative to its back (i.e. narrow MTZ), which is reflected by the sharp slope in the curve shown by the smaller sample.

Two factors that greatly affect the MTZ formation are the gas residence time in the bed and the bed length to diameter ratio (L/D). High L/D and high gas residence time lead to narrow MTZ, hence faster adsorption kinetics and bigger capacity at the breakthrough point, as the adsorbate will be in contact with the adsorbent bed for enough time. In this case, the larger sample (48 g) has lower L/D (1.26) than the smaller sample (1.59), but higher gas residence time (14.51 s) compared to the smaller sample (7.98 s). Since low capacity at the breakthrough point is recorded for the larger sample, it seems the enhancement in the gas residence time is outweighed by the decrease in the L/D ratio.

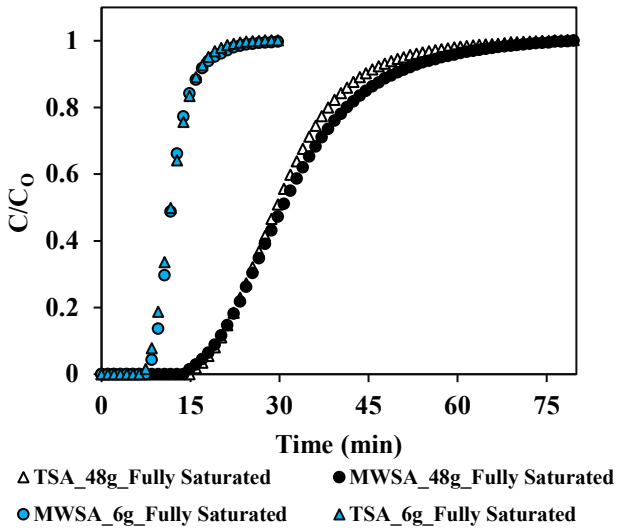

Figure 4. Norit R: CO_2 breakthrough curve profiles during MWSA and TSA (adsorption with saturation) with large (48 g) and small mass (6 g). Feed in the adsorption step: wet flue gas (CO_2/N_2 + Moisture: 15/85 + 15 % RH).

To understand the drop in breakthrough capacity observed in the unsaturated tests in the larger mass, the length of the unused bed (LUB) at the breakthrough point was evaluated for the two sample masses and results are summarised in Table 7. LUB represents the part of the mass transfer zone where adsorbent is not used at the time of breakpoint and is calculated as follows:

$$LUB\ (cm) = L \cdot (1 - Wt_b / Wt_s) \qquad \text{(Eq. 13)}$$

where, Wt_s (g/g) is the total mass of CO_2 captured per gram of adsorbent at saturation, Wt_b (g/g) is the total mass of CO_2 captured per gram of adsorbent at the breakthrough time, and L (cm) is the total bed length.

A small value of LUB implies efficient utilisation of the bed. It is apparent from the results that the 6 g sample has the lower fraction of unused bed which is 45 % of the total, hence it explains the higher CO_2 uptake capacity exhibited. The LUB for the 48 g is 3.49 cm which amounts to 60 % length of the unused bed. As mentioned earlier, increasing the feed flow rate fourfold (i.e. from 100 to 400 ml/min) did not decrease the gas residence time, however, the L/D is reduced in the larger sample, which seems to have impacted the flow path and distribution of the gas in the bed, hence led to larger LUB and lower uptake capacity at the breakthrough point.

Table 7. LUB for 6 and 48 g of Norit R. Total feed gas: 100 and 400 ml/min (unsaturated cycles)

Sample size	**Wt_s**	**Wt_b**	**L (cm)**	**LUB (%)**	**LUB (cm)**
Mass = 6 g	0.037	0.020	3.50	45	1.57
Mass= 48 g	0.037	0.015	5.82	60	3.49

In Figure 5 a-d, the adsorption and desorption steps along with their corresponding temperature profiles are depicted for both masses. Desorption profiles for the large mass follow a similar pattern as in the small mass. In the large sample, CO_2 desorbed peaks start to emerge 10 and 15 mins from the start of the regeneration (heating) process with MWSA and TSA, respectively. In the small sample, on the other hand, they emerge after 18 mins with MWSA and 23 mins with TSA. This corresponds to a sooner detection of the first desorbed CO_2 peak with the larger sample (8 mins earlier) compared to the small one, in both heating modes. This earlier appearance of the CO_2 desorption peak in the large sample is mainly ascribed to the increased purge gas flow rate, which was raised fourfold (i.e. from 20 to 80 Nml/min) to speed up the regeneration time. The peaks in TSA appear 5 mins after that of MWSA, which coincides with the observed in the small mass. This means that the regeneration with MWSA is faster than with TSA. The gap in peak concentration between TSA and MWSA for the 48 g is 12 % v/v, not far from the 14 % v/v difference found between them in the 6 g sample.

The results highlight that microwave heating offers enhanced CO_2 desorption at shorter times (bigger CO_2 concentration detected in the reactor outlet at earlier times). The regeneration in the TSA was found 32 % longer compared to MWSA.

Displayed in Figure 5 c are the temperature profiles recorded during the 7 mins of microwave heating of both sample masses. The adsorbents reached the target temperature within 2 mins in both masses, however, an initial slower heating rate in the first 55 seconds can be seen in the 48 g sample, followed by a fast rate which ended up in a bigger overshoot than the 6 g sample, almost 10 ℃ above the set temperature due to the higher temperature inertia in this case. It took 2 mins to correct for the temperature overshoot and the undershoot that followed to stabilise around the target temperature (100 ± 3 ℃). In the case of TSA, the heating rate for the smaller sample was found two times faster than the large sample until 93 ℃ was reached (46.6 and 23.3 ℃/min respectively), after that they are both kept at 7 ℃/min for 1 min to achieve the target temperature (100 ± 3 ℃).

There is clear evidence of microwave heating advantage over conventional heating in the results observed in Figure 5 c and d. With microwave heating, the temperature profiles followed by both the 6 and 48 g samples overlapped. This means that heating a larger mass of adsorbent using microwave radiation overcomes the heat transfer limitation observed in conventional heating for the larger sample mass (Fig 6 d). Additionally, another advantage observed when using microwave heating for regeneration is the increased desorbed CO_2 concentration at any time with MWSA compared to TSA, regardless of the sample size, and the reduced regeneration time by almost 1/3 (32 %) in MWSA compared to TSA. This is a clear indication of the benefits of process intensification features which can be obtained from the use of microwave heating for post-combustion carbon capture

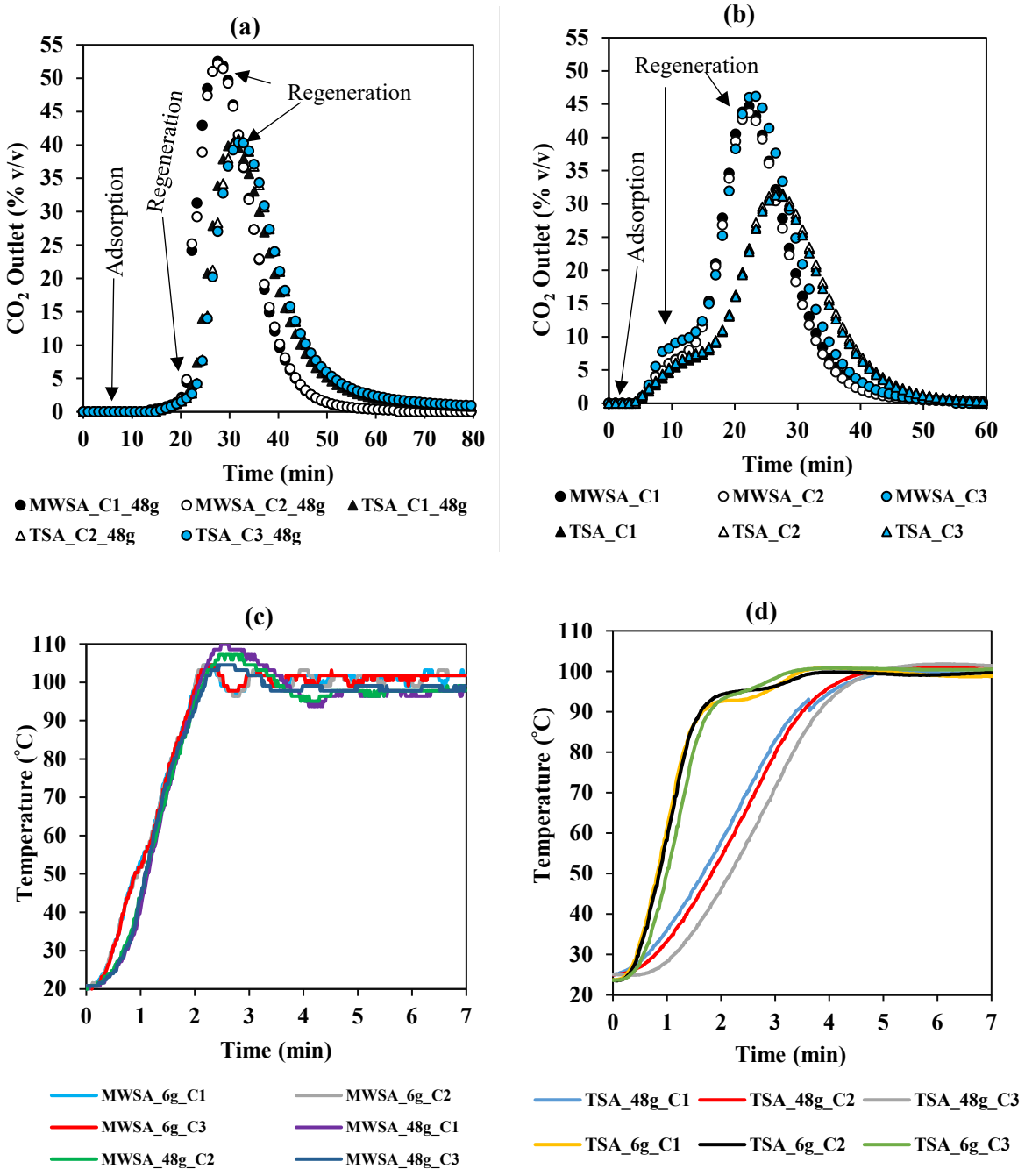

Figure 5. Norit R: adsorption and desorption profiles with MWSA and TSA for the 48 g (a), and 6 g (b). Temperature regeneration profiles for both masses under MWSA (c) and TSA (d). Adsorption feed: wet flue gas (CO_2/N_2 + Moisture, 15/85 + 15 % RH). C_1, C_2 and C_3 stand for cycle 1, cycle 2 and cycle 3 respectively.

3.5.2 Effect of sample size on CO_2 productivity, purity, and recovery: MWSA *vs* TSA

Figure 6 displays the purity, recovery, and productivity for MWSA and TSA in two sample masses of Norit R (6 and 48 g). Overall, all three parameters are higher with MWSA than TSA in both sample masses.

Overall, productivity is smaller for the 48 g sample compared to the 6 g sample in both regeneration modes. With MWSA, the average productivity is at 814.29 mol/(kg h) for the 6 g sample compared to 493.33 mol/(kg h) for the 48 g. With TSA, average productivities are 612.77 and 317.14 mol/(kg h) for the small and large samples respectively. These results also show that average productivities are smaller under conventional heating compared to microwave heating for both sample masses. For the 6 g sample, productivity is 25 % lower in TSA than in MWSA, where for the 48 g sample, it is 36 % smaller in TSA compared to MWSA.

The improved productivity under MWSA is mainly due to the shorter regeneration time/cycle time needed when microwave heating was used, as well as enhanced uptake capacity after cycles observed with MWSA. The enhanced capacity is due to better regeneration achieved in MWSA under the same operating conditions, leading to bigger capture in subsequent cycles. Additionally, the smaller productivity in the larger sample is expected. Firstly, the capacity is lower due to the bigger length of the unused bed (LUB)and the lower L/D compared to that used for the small sample. Secondly, the cooling period is comparatively longer in the larger mass because of slower heat loss from the increased adsorbent mass leading to increased cycle time, hence lower productivity.

Purity is over 98 % in all cases in both sample masses, although marginally higher in MWSA. For the small mass, purity of 99.6 % with MWSA and 98.4 % with TSA were obtained, where for the large mass, 99.3 and 98.9 % were obtained in the same order.

Recovery is also higher in MWSA in both sample masses. The difference in the recovered amount of CO_2 is especially high for the small sample, with 96.1 % in MWSA compared to 75.1 % in TSA. In the case of the large mass, 98.6 and 96.3 % of CO_2 recovery were recorded for MWSA and TSA, respectively. The difference in recovery between the TSA and MWSA for the 6 g is that both the CO_2 capture capacity and the desorbed CO_2 were smaller in TSA because of a lack of full regeneration in

the previous cycle. Consequently, as the total feed used was the same for both regeneration strategies, a smaller value is obtained for TSA. In the large sample, $Qfeed_{CO2}$ was low (16.28 mg/g) and exactly equal in both processes and the desorbed amount was the same, hence, the CO_2 recovery presented a very close value with MWSA and TSA. Variations observed in these factors between the 3 cycles measured for the same swing adsorption process are negligible, which could be an indication that these performance parameters are representative and stable in cyclic operation.

In summary, better performances of the three parameters (i.e. productivity, purity, recovery) were obtained under MWSA as opposed to TSA in both sample sizes. Nonetheless, productivity is reduced with an increase in sample size in both regeneration modes, whereas purity is not affected much by the change in sample size. Recovery was enhanced with an increase in mass, especially in the TSA.

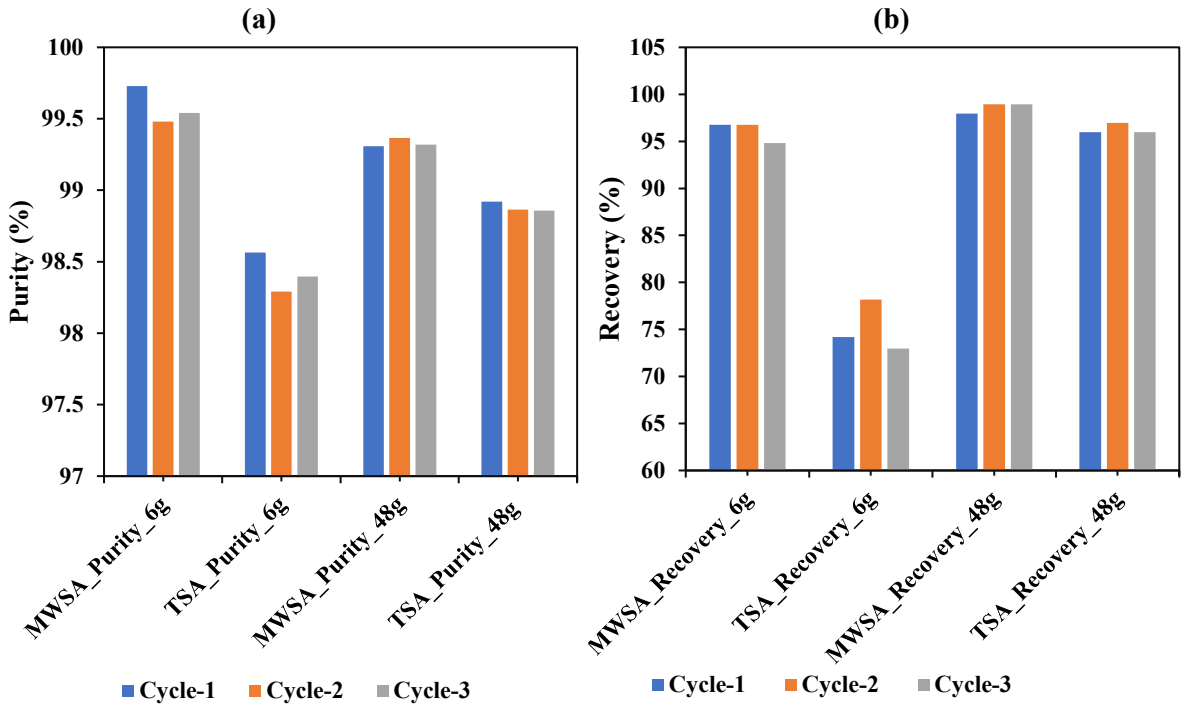

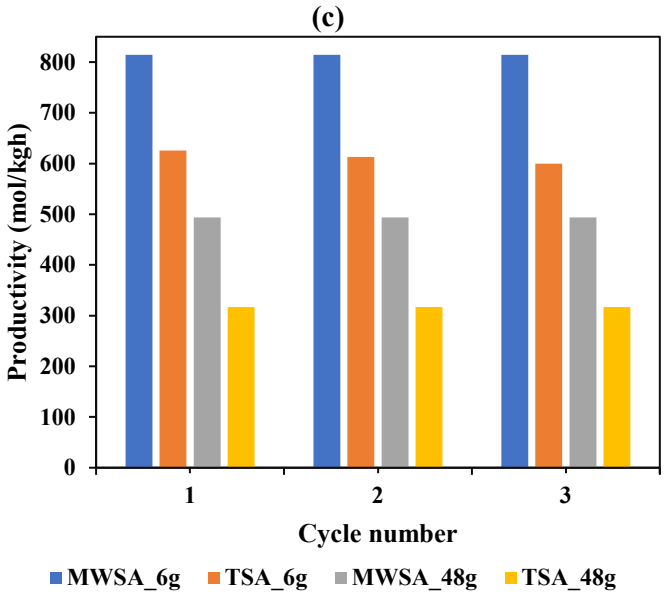

Figure 6. CO_2 purity (a), recovery (b), and productivity (c) for Norit R. C_1, C_2 and C_3 stand for cycle 1, cycle 2 and cycle 3 respectively.

3.5.3. Effect of sample size on CO_2 regeneration extent: MWSA *vs* TSA

The effect of sample mass on regeneration time required to achieve the same CO_2 regeneration percentage was assessed and compared for 6 and 48 g of Norit R (see Figure 7 and Table 8). With both sample sizes, a higher fraction of CO_2 is released with microwave-assisted regeneration than with conventionally assisted regeneration for the same desorption period. The difference is especially pronounced in the large sample.

Under MWSA, the time needed to obtain 50, 80, 90, and 99 % regeneration was smaller in the large sample compare to the small one (10, 16, 19, and 32 mins in the 48 g sample, and 17, 22, 25, and 39 mins in the 6 g one, respectively). With TSA, CO_2 is removed at a close rate for the first 5 mins in both samples (0.80 %/min for the 6 g and 0.55 %/min for the 48 g). Between the 5^{th} and 30^{th} min, a higher regeneration percentage (average: 53 % for 48 g and 39 % for 6 g) is achieved with the larger sample. Nevertheless, removing the last 10 % of the adsorbate took longer in large mass (i.e 12 mins for 6 g compared to 27 mins in 48 g). However, the 4.5 times longer period in the larger sample is not proportional to the 8 times bigger sample. Additionally, compared to TSA, it took a shorter time with MWSA (5, 7, 11, and 25 mins less time) to achieve 50, 80, 90, 99 % regeneration respectively for the

48 g, whereas, for the 6 g sample, regeneration time was 4, 5, 7, and 5 mins less in MWSA as opposed to TSA in that same order.

Overall, the results show that MWSA brings about a reduction in regeneration time in both sample masses, and with an increase in sample size, the reduction is even bigger. For instance, regeneration time was reduced by 34.37 % in the MWSA to achieve a 90 % regeneration compared to TSA. This is a good indication that a scale-up process would have further advantages with microwave compared to conventional regeneration in a CCUS installation. In removing the last 10 % of CO_2 remaining in the adsorbent, a similar time was needed in MWSA for both masses (13 mins for the 48 g compared to 14 mins for the 6 g), whereas with TSA, it was almost 2 times longer in the large mass (12 mins for 6 g as opposed to 27 mins for 48 g), which shows the clear heat transfer limitation when the regeneration is assisted with conventional heating.

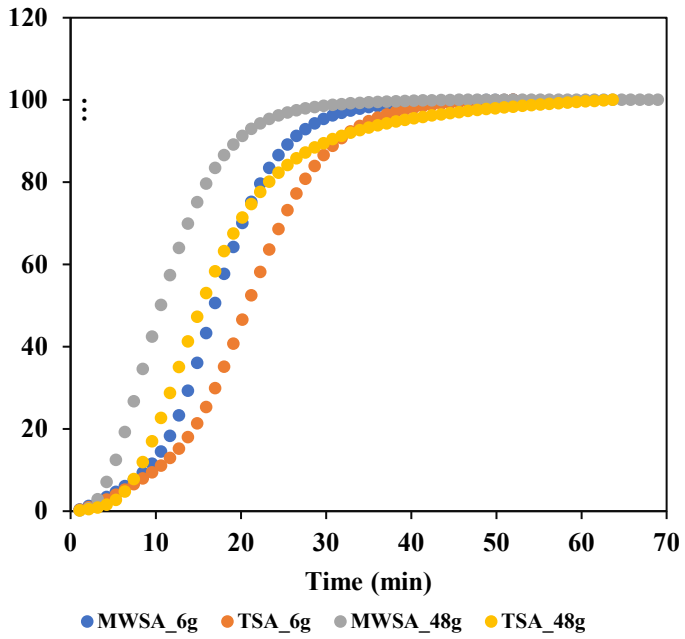

Figure 7. Effect of the sample mass on the CO_2 desorption profile (in percentage of CO_2 desorbed with respect to the total regenerated) from Norit R, with MWSA and TSA (average of the three cycles). Adsorption feed: CO_2/N_2 + Moisture (15/85 + 15 % RH).

Table 8: Time needed to achieve 50, 80, 90, and 99 % regeneration with TSA and MWSA for 6 and 48 g samples of Norit R

Adsorbent	Sample size		t_{50}	t_{80}	t_{90}	t_{99}
Norit R	6 g	MWSA	17	22	25	39
		TSA	21	27	32	44
	48 g	MWSA	10	16	19	32
		TSA	15	23	30	57

4. Conclusions

This work presents an in-depth comparative analysis of the dynamic performance of CO_2 capture adsorbents with an unconventional microwave regeneration technology and its comparison with conventional regeneration. The results not only affirm the viability of microwave heating for adsorbents regeneration but also present evidence of its benefits over conventional thermal heating. Assessment on the working capacity of Norit R and 13X in two feed gas conditions (dry and wet), showed advantages of MWSA over TSA in all cases. For Norit R, the working capacity was 39.68 % higher with the wet feed gas and 9.36 % higher with the dry under MWSA compared to TSA. For 13X, the working capacity was 24.23 and 20.39 % higher with wet and dry feed gas respectively under MWSA as opposed to TSA. The superior performance in microwave heating seen in both adsorbents in each gas condition can be attributed to a better regeneration realised under MWSA compared to TSA.

In assessing purity, productivity, and recovery, greater performance was achieved under MWSA for each of the three parameters in both adsorbents. The productivity achieved in MWSA was 25 % higher than that achieved in TSA for Norit R. The productivity was also higher (by 27 %) in MWSA than in TSA for 13X. High and stable purity was obtained in both heating modes, but marginally better in MWSA at 99.3 % average, compared to 98.5 % average in TSA. Recovery varied between the adsorbents, cycles, and heating modes. It was found to be 21 and 15 % higher in MWSA than TSA for Norit R and 13X, respectively.

In evaluating the process of CO_2 desorption from the adsorbents, the regeneration data were fitted to three kinetic models. From this, Avrami's model adequately predicted the desorption proportion of CO_2 as a function of time, signifying the applicability of the model to the desorption process mechanism to some extent. Finally, the result obtained from the increased sample size indicates that microwave regeneration could offer potential benefits over conventional regeneration in an up-scaled process, leading to enhanced performance such as less time to reach the regeneration temperature, and reduction in regeneration time.

Author's contribution: conceptualization C.F.M; methodology: C.F.M and M.Y.; investigation and data curation: M.Y and C.F.M; writing—original draft preparation: M.Y and C.F.M.; writing—review and editing: C.F.M., M.Y., S.B. and W.A.; visualization and funding acquisition: C.F.M; supervision: C.F.M. and W.A. All authors have read and agreed to the published version of the manuscript.

Acknowledgment: this work was carried out thanks to the financial support provided by the School of Engineering, University of Aberdeen through the fully-funded PhD Scholarship awarded to the lead supervisor Dr C. F. Martín, and also thanks to the financial support received from The Development Trust for the acquisition of FlexiWave and micro-GC, employed in this project. Mr Mohamud Yassin acknowledges the School of Engineering, University of Aberdeen for the financial support provided through the PhD Scholarship. Finally, authors thank Cabot for supplying free samples of Norit R2030CO_2.

Conflicts of Interest: The authors declare no conflict of interest

5. References

[1] IEA, CO_2 emissions from fuel combustion, OECD/IEA. (2016) 9. https://doi.org/10.1787/co2_fuel-2016-en.

[2] A. Ruzmaikin, A. Byalko, On the relationship between atmospheric carbon dioxide and global temperature, American Journal of Climate Change. 4 (2015) 181–186. https://doi.org/10.4236/ajcc.2015.43014.

[3] IPCC, AR5 - Working group 3, mitigation of climate change - contribution of working group III, 2014.

[4] M. Delmotte, V., P. Zhai, A. Pirani, S.L. Connors, C. Péan, S. Berger, N. Caud, Y. Chen, L. Goldfarb, M.I. Gomis, and B.Z. Huang, K. Leitzell, E. Lonnoy, J.B.R. Matthews, T.K. Maycock, T. Waterfield, O. Yelekçi, R. Yu, IPCC, 2021: Summary for Policymakers. In: Climate Change 2021: The Physical Science Basis. Contribution of Working Group I to the Sixth Assessment Report of the Intergovernmental Panel on Climate Change, 2021.

[5] Department of Energy and Climate Change, CCS Roadmap. supporting deployment of carbon capture and storage in the UK, 2012. https://doi.org/URN 12D/016.

[6] M.R.M. Abu-Zahra, Z. Abbas, P. Singh, P. Feron, Carbon Dioxide Post-Combustion Capture: Solvent Technologies Overview, Status and Future Directions, Materials and Processes for Energy: Communicating Current Research and Technological Developments. (2013) 923–934.

[7] W. Zhang, C. Sun, C.E. Snape, R. Irons, S. Stebbing, T. Alderson, D. Fitzgerald, H. Liu, Process simulations of post-combustion CO_2 capture for coal and natural gas-fired power plants using a polyethyleneimine/silica adsorbent, International Journal of Greenhouse Gas Control. 58 (2017) 276–289. https://doi.org/10.1016/j.ijggc.2016.12.003.

[8] K. Thambimuthu, M. Soltanieh, J.C. Abanades, R. Allam, O. Bolland, J. Davison, P. Feron, F. Goede, A. Herrera, M. Iijima, D. Jansen, I. Leites, P. Mathieu, E. Rubin, D. Simbeck, K. Warmuzinski, M. Wilkinson, R. Williams, M. Jaschik, A. Lyngfelt, R. Span, M. Tanczyk, Capture of CO_2, IPCC Special Report on Carbon Dioxide Capture and Storage. (2005) 105–178.

[9] E. Meloni, M. Martino, P. Pullumbi, F. Brandani, V. Palma, Intensification of TSA processes using a microwave-assisted regeneration step, Chemical Engineering and Processing - Process Intensification. 160 (2021) 108291. https://doi.org/10.1016/j.cep.2020.108291.

[10] F. Bougie, D. Pokras, X. Fan, Novel non-aqueous MEA solutions for CO_2 capture, International Journal of Greenhouse Gas Control. 86 (2019) 34–42. https://doi.org/10.1016/j.ijggc.2019.04.013.

[11] P.A. Webley, J. Zhang, Microwave assisted vacuum regeneration for CO_2 capture from wet flue gas, Adsorption. 20 (2014) 201–210. https://doi.org/10.1007/s10450-013-9563-y.

[12] K.Y. Foo, B.H. Hameed, A cost effective method for regeneration of durian shell and jackfruit peel activated carbons by microwave irradiation, Chemical Engineering Journal. 193–194 (2012) 404–409. https://doi.org/10.1016/j.cej.2012.04.055.

[13] I. Polaert, L. Estel, R. Huyghe, M. Thomas, Adsorbents regeneration under microwave irradiation for dehydration and volatile organic compounds gas treatment, Chemical Engineering Journal. 162 (2010) 941–948. https://doi.org/10.1016/j.cej.2010.06.047.

[14] Y.T. Chen, Y.P. Huang, C. Wang, J.G. Deng, H.C. Hsi, Comprehending adsorption of methylethylketone and toluene and microwave regeneration effectiveness for beaded activated

carbon derived from recycled waste bamboo tar, Journal of the Air and Waste Management Association. 70 (2020) 616–628. https://doi.org/10.1080/10962247.2020.1742247.

[15] Y. Lv, J. Sun, G. Yu, W. Wang, Z. Song, X. Zhao, Y. Mao, Hydrophobic design of adsorbent for VOC removal in humid environment and quick regeneration by microwave, Microporous and Mesoporous Materials. 294 (2020) 109869. https://doi.org/10.1016/j.micromeso.2019.109869.

[16] S. Ito, H. Huang, F. Watanabe, H. Yuan, M. Hasatani, N. Kobayashi, Heat transfer during microwave-assisted desorption of water vapor from zeolite packed bed, Drying Technology. 30 (2012) 1707–1713. https://doi.org/10.1080/07373937.2012.714825.

[17] Q.S. Liu, P. Wang, S.S. Zhao, W. Zhang, Treatment of an industrial chemical waste-water using a granular activated carbon adsorption-microwave regeneration process, Journal of Chemical Technology and Biotechnology. 87 (2012) 1004–1009. https://doi.org/10.1002/jctb.3720.

[18] A.Dyer, Encyclopedia of materials: science and technology (second edition), Zeolites. (2006) 1–5.

[19] M.M. Yassin, J.A. Anderson, G.A. Dimitrakis, C.F. Martín, Effects of the heating source on the regeneration performance of different adsorbents under post-combustion carbon capture cyclic operations. A comparative analysis, Separation and Purification Technology. 276 (2021) 119326. https://doi.org/10.1016/j.seppur.2021.119326.

[20] Honeywell, HIH-4000-003, (2010).

[21] F. Raganati, R. Chirone, P. Ammendola, CO_2 capture by temperature swing adsorption: working capacity as affected by temperature and CO_2 partial pressure, Industrial and Engineering Chemistry Research. 59 (2020) 3593–3605. https://doi.org/10.1021/acs.iecr.9b04901.

[22] D. Marx, L. Joss, M. Hefti, R. Pini, M. Mazzotti, The role of water in adsorption-based CO_2 capture systems, Energy Procedia. 37 (2013) 107–114. https://doi.org/10.1016/j.egypro.2013.05.090.

[23] J.M. Kolle, M. Fayaz, A. Sayari, Understanding the effect of water on CO_2 adsorption, Chemical Reviews. 121 (2021) 7280–7345. https://doi.org/10.1021/acs.chemrev.0c00762.

[24] I. Durán, F. Rubiera, C. Pevida, Separation of CO_2 in a solid waste management incineration facility using activated carbon derived from pine sawdust, Energies. 10 (2017). https://doi.org/10.3390/en10060827.

[25] Y. Sun, Y. Wang, Y. Zhang, Y. Zhou, L. Zhou, CO_2 sorption in activated carbon in the presence of water, Chemical Physics Letters. 437 (2007) 14–16. https://doi.org/10.1016/j.cplett.2007.02.008.

[26] Almaz S. Jalilov, Y. Li, C. Kittrell, J.M. Tou, Increased CO_2 selectivity of asphalt-derived porous carbon through introduction of water into pore space, Nature Energy. (2017).

[27] Y. Chen, Z. Qiao, J. Huang, H. Wu, J. Xiao, Q. Xia, H. Xi, J. Hu, J. Zhou, Z. Li, Unusual moisture-enhanced CO_2 capture within microporous PCN-250 frameworks, ACS Applied Materials and Interfaces. 10 (2018) 38638–38647. https://doi.org/10.1021/acsami.8b14400.

[28] D. Xu, P. Xiao, J. Zhang, G. Li, G. Xiao, P.A. Webley, Y. Zhai, Effects of water vapour on CO_2 capture with vacuum swing adsorption using activated carbon, Chemical Engineering Journal. 230 (2013) 64–72. https://doi.org/10.1016/j.cej.2013.06.080.

[29] J. Rodríguez-Mirasol, J. Bedia, T. Cordero, J. Rodríguez, Influence of water vapor on the adsorption of VOCs on lignin-based activated carbons, Separation Science and Technology. 40 (2005) 3113–3135. https://doi.org/10.1080/01496390500385277.

[30] M.D. Turner, R.L. Laurence, W.C. Conner, K.S. Yngvesson, Microwave radiation's influence on sorption and competitive sorption in zeolites, AIChE Journal. 46 (2000) 758–768. https://doi.org/10.1002/aic.690460410.

[31] A. Borhan, S. Yusup, J.W. Lim, P.L. Show, Characterization and modelling studies of activated carbon produced from rubber-seed shell using KOH for CO_2 adsorption, Processes. 7 (2019). https://doi.org/10.3390/pr7110855.

[32] H. Moussout, H. Ahlafi, M. Aazza, H. Maghat, Critical of linear and nonlinear equations of pseudo-first order and pseudo-second order kinetic models, Karbala International Journal of Modern Science. 4 (2018) 244–254. https://doi.org/10.1016/j.kijoms.2018.04.001.

[33] Y.S. Ho, G. McKay, Sorption of dye from aqueous solution by peat, Chemical Engineering Journal. 70 (1998) 115–124. https://doi.org/10.1016/S1385-8947(98)00076-X.

[34] M.A. Hubbe, S. Azizian, S. Douven, Implications of apparent pseudo-second-order adsorption kinetics onto cellulosic materials: a review, BioResources. 14 (2019) 7582–7626. https://doi.org/10.15376/biores.14.3.7582-7626.

[35] Q. Liu, J. Shi, S. Zheng, M. Tao, Y. He, Y. Shi, Kinetics studies of CO_2 adsorption/desorption on amine-functionalized multiwalled carbon nanotubes, Industrial and Engineering Chemistry Research. 53 (2014) 11677–11683. https://doi.org/10.1021/ie502009n.

[36] Y. Teng, Z. Liu, G. Xu, K. Zhang, Desorption kinetics and mechanisms of CO_2 on amine-based mesoporous silica materials, Energies. 10 (2017). https://doi.org/10.3390/en10010115.

[37] S. Karka, S. Kodukula, S. V. Nandury, U. Pal, Polyethylenimine-modified zeolite 13X for CO_2 capture: adsorption and kinetic studies, ACS Omega. 4 (2019) 16441–16449. https://doi.org/10.1021/acsomega.9b02047.